Journal of Bone and Mineral Metabolism (2021) 39:126–138
https://doi.org/10.1007/s00774-020-01122-0

ORIGINAL ARTICLE

SDF-1 mediates mesenchymal stem cell recruitment and migration via the SDF-1/CXCR4 axis in bone defect

Heli Zhang[1] · Xijing Li[2] · Junfeng Li[3] · Lili Zhong[4] · Xue Chen[5] · Si Chen[6]

Received: 25 April 2019 / Accepted: 27 June 2020 / Published online: 20 October 2020

Abstract

Introduction Recent studies have indicated the potential of stem cell therapy in combination with cytokines to restore the bone repair via migration and homing of stem cells to the defected area. The present study aimed to investigate the mobilization and recruitment of mesenchymal stem cells (MSCs) in response to SDF-1.

Materials and Methods Herein, the knockout rat model of the bone defect (BD) was treated with the induced membrane technique. Then, wild type Wistar rats and SDF-1-knockout rats were selected for the establishment of BD-induced membrane (BD-IM) models and bone-graft (BG) models. The number of MSCs was evaluated by flow cytometry, along with the expression pattern of the SDF-1/CXCR4 axis as well as osteogenic factors was identified by RT-qPCR and Western blot analyses. Finally, the MSC migration ability was assessed by the Transwell assay.

Results Our data illustrated that in the induced membrane tissues, the number of MSCs among the BD-IM modeled rats was increased, whereas, a lower number was documented among BG modeled rats. Besides, we found that lentivirus-mediated over-expression of SDF-1 in BG modeled rats could activate the SDF-1/CXCR4 axis, mobilize MSCs into the defect area, and up-regulate the osteogenic proteins.

Conclusions Collectively, our study speculated that up-regulation of SDF-1 promotes the mobilization and migration of MSCs through the activation of the SDF-1/CXCR4 signal pathway.

Keywords Stromal cell-derived factor-1 · SDF-1/CXCR4 axis · Bone defect · Bone graft · Induced membrane technique

Heli Zhang, Xijing Li have contributed equally to this work.

✉ Xue Chen
chenxue_drchen@126.com

✉ Si Chen
chen_chensi@163.com

[1] Department of Outpatient, The Second Hospital of Jilin University, Changchun 130041, People's Republic of China

[2] Department of Emergency, The Second Hospital of Jilin University, Changchun 130041, People's Republic of China

[3] Department of Clinical Laboratory, The Second Hospital of Jilin University, Changchun 130041, People's Republic of China

[4] Jilin Provincial Key Laboratory On Molecular and Chemical Genetic, The Second Hospital of Jilin University, Changchun 130041, People's Republic of China

[5] Department of Orthopedics, The Second Hospital of Jilin University, No. 218, Ziqiang Street, Nanguan District, Changchun 130041, Jilin, People's Republic of China

[6] Department of Geriatric Medicine, The Second Hospital of Jilin University, No. 218, Ziqiang Street, Nanguan District, Changchun 130041, Jilin, People's Republic of China

Introduction

An array of factors have been identified as the causative reason for bone defect (BD), including tumors, infection, and trauma, among which trauma accounts for the highest prevalence [1, 2]. Patients suffering from BD may experience extensive impairment in function due to the presence of a lesion in the vicinity as well as a poor quality of life [3]. Currently, the clinically approved supplies for BD treatment comprise predominantly of autologous bone and allogenic bone, both of which have limitations and shortcomings, such as delayed fracture healing, possible blood loss, and poor anti-infection ability [4]. With acknowledgment of the advancements made for the development of new therapeutic strategies, induced membrane techniques in the field of tissue engineering have emerged as a promising surgical alternative [5]. The mechanism of this technique incorporates filling the BD with a cement spacer, triggering a reaction to a foreign object [6]. Furthermore, the involvement of mesenchymal stem cells (MSCs), in particular, has also been reported in the processes of bone building [5], possibly due to the intrinsic trophic

factors released by MSCs. Moreover, bone marrow-derived MSCs (BMSCs) can differentiate into multiple types of cells including fat, bone, and cartilage, as well as migrating to injury sites to facilitate tissue repair.

The trophic factors released by MSCs may be responsible for its involvement. Moreover, MSCs can conceivably respond to certain mediators, such as stromal cell-derived factor 1 (SDF-1) [7]. SDF-1, also known as C-X-C motif chemokine ligand 12 (CXCL12), forms part of the alpha-chemokine family with documented expression in a variety of cells within the bone marrow [8, 9]. C-X-C motif chemokine receptor 4 (CXCR4), a G-protein coupled receptor with 7 transmembrane domains, is the receptor of SDF-1, whose expression has also been reported in various cell types [8, 10, 11]. Fakhari et al. asserted that the migration potential of BMSCs was amplified by the SDF-1/CXCR4 axis after *Helicobacter pylori* infection [12]. Interestingly, SDF-1 contributes to cartilage defect repair through recruitment of BMSCs and induces its chondrogenic differentiation [13]. The SDF-1/CXCR4 system has been implicated during the repair of the femoral bone damage by impacting various stem cell populations such as mesenchymal stem cells and hematopoietic stem cells [14]. Hence, during the current study, we established BD-induced membrane (BD-IM) and bone-graft (BG) models in Wistar rats and SDF-1-knockout rats in an attempt to investigate the effects of SDF-1/CXCR4 axis on the function of MSCs.

Materials and methods

Ethics statement

The study was conducted under the approval of the Animal Ethics Committee of the Second Hospital of Jilin University. All rat experiments were conducted in strict accordance with the Guidelines for the Care and Use of Laboratory Animals proposed by the National Institutes of Health.

Experimental animals

A total of 100 male specific pathogen free Wistar rats (weight 190 ± 10 g; age 9 weeks) were obtained from Beijing Vital River Laboratory Animal Technology Co., Ltd. (Beijing, China) for the experiment. Another batch of 60 SDF-1-knockout Wistar rats (weight 190 ± 9 g; age 9 weeks) was purchased from Shanghai Bioray Laboratories Inc., (Shanghai, China). All rats were prepared for BD-IM model and bone-graft (BG) model construction.

Establishment of BD-IM and BG models and rat grouping

The 100 Wistar rats along with 60 SDF-1-knockout rats were fasted for 4–6 h prior to operative procedures. Next, the rats were anaesthetized by administrating an intraperitoneal injection using 3% pentobarbital sodium (1 ml/kg). Skin preparation was performed in a conventional manner on the left femur. A 2-cm incision was made on the outer thigh region, and the surrounding muscle and soft tissues were isolated by blunt dissection in order to expose the middle segment of the femur. The persisting BD (10 mm) was obtained by conducting a mini-plate fixation. Next, the periosteum was completely cleared. Cylinder-shaped PMMA bone cement (Simplex P, Howmedica Osteonics Corp., NJ, USA) of 3 × 10 mm was used to fill the BD and wrap both ends. Surgical incisions were sutured layer-by-layer and dressed using sterile auxiliary materials. At the 0- and 24-h post-operation points, penicillin (2×10^5 U/kg) was administered intramuscularly as a precaution to stave off infection. Upon wakening up, each rat was allowed to move in a temperature controlled cage (25 ± 2 °C) with free access to food and water. The BD-IM model was subsequently established [15]. A total of 96 successfully modeled Wistar rats as well as the additional 60 SDF-1-knockout rats were selected for further experimentation.

Rats in the BD-IM model were randomly selected and grouped into SDF-$1^{-/-}$ group (SDF-1 knockout rats, $n = 21$), SDF-1 group (Wistar rats implanted with BMSCs overexpressing SDF-1, $n = 21$) and control group (Wistar rats, $n = 21$). As for Wistar rats in the SDF-1 group, MSCs overexpressing SDF-1 (Shanghai GenePharma Co., Ltd., Shanghai, China) were constructed by infection with lentiviral vector overexpressing SDF-1. The BMSCs overexpressing SDF-1 were implanted into the bone marrow prior to suturing of the surgical incisions.

After 4 weeks, the bone cement was removed from the remaining 54 Wistar rats and 39 SDF-1-knockout rats. Intramembrane implantation of autogenous cancellous bone was performed to establish the BG model [16]. Finally, 49 Wistar rats and 34 SDF-$1^{-/-}$ rats were successfully modeled, among which rats were randomly selected and then grouped into BG SDF-$1^{-/-}$ group (SDF-1-knockout rats undergone BG, $n = 21$), BG SDF-1 group (Wistar rats delivered with BMSCs overexpressing SDF-1 and undergone BG, $n = 21$), and BG control group (Wistar rats undergone BG, $n = 21$).

Sample collection

Bone marrow, peripheral blood, and induced membrane tissues were collected from rats of the BD-IM and BG models on days 1, 3, 7, 10, 14, 28, and 56 post-operation. Three individual rats in each group (the SDF-$1^{-/-}$, SDF-1, and control groups) were euthanatized by CO_2 inhalation at each time point. Blood extraction was conducted from the rat heart using a heparinized syringe. Next, the rats were soaked in 75% alcohol for 10 min for sterilization. Bone in the defect area was withdrawn in sterile conditions with removal of

soft tissues that were attached on the surface cleaned, followed by phosphate-buffered solution (PBS) washing. The metaphysis on both ends was removed using a pair of scissors to further expose the bone marrow cavity, which was then rinsed using α-minimum essential medium (α-MEM) containing 10% fetal bovine serum (FBS). The bone marrow was repeatedly triturated using a syringe with a NO.5 needle and collected. The bone cement was collected after euthanasia. The surrounding semipermeable membrane tissue was cut into slices of 3–4 mm using sterile scissors. Fragments of tissue were rinsed in calcium and magnesium-free balanced salt solution. The supernatant was then discarded. Following 2–3 subsequent rinses, the tissue was placed over ice. The remaining supernatant was abandoned. The aforementioned procedure was conducted on the sample collection from rats in the BG model.

MSC isolation by density gradient centrifugation

MSCs in the peripheral blood, induced membrane, and bone marrow were isolated and extracted from rats of the BD-IM and BG models. The extracted bone marrow tissues from the femur of rats were triturated repeatedly with DMEM/F12 basal medium, after which the single cell suspension was harvested and then subjected to centrifugation in a horizontal centrifuge. The cells were then seeded in a culture bottle (25 ml) supplemented with DMEM/F12 complete medium (containing 100 IU/ml penicillin, 100 g/ml streptomycin, and 10% FBS) at a density of 4×10 cells/cm^2 and then cultured under saturated humidity atmosphere of 5% CO_2 at 37 °C. The medium was changed after 48–72 h and then renewed every 3 days. Morphological changes and growth of cells were observed under an inverted microscope daily. When the cell confluence reached 80–90%, the cells were rinsed with PBS and then detached using 0.02% ethylenediaminetetraacetic acid/0.25% trypsin (volume ratio of 1:1) at 37 °C for 35 min, which was blocked upon addition of the serum. The cell suspension was collected and centrifuged following the trituration. Next, the cell density was adjusted to 1×10 cells/cm^2 after re-suspension in DMEM/F12 complete medium containing 10% FBS. Next, the cells were inoculated in a culture bottle (25 cm^2) and passaged at a ratio of 1:2. MSCs were extracted from peripheral blood according to the following procedures: Blood was collected from the heart of experimental rats using a heparinized sterile injection. After the removal of erythrocytes, the isolated monocytes were re-suspended in 0.125% Tris-NH_4Cl buffer solution. Monocytes in the peripheral blood were extracted using a filter mesh. MSCs were collected from an induced membrane tissue as follows: rats were sacrificed and the bone cement was removed accordingly. The surrounding semipermeable membrane tissue was then cut into slices of 3–4 mm using sterile scissors. Fragments of the tissue were rinsed in calcium and magnesium-free balanced salt solution. The supernatant was discarded. After 2–3 subsequent rinses, the tissue was placed over ice. The remaining supernatant was discarded. Then, every 100 mg of tissue was incubated with 1 ml of trypsin (0.25%) dissolved in calcium and magnesium-free balanced salt solution at 4 °C for 6–18 h until penetrance of all trypsin without tryptic activity was achieved. Trypsin in the fragments of tissues was abandoned. Fragments of tissue containing left trypsin were incubated at 37 °C for 20–30 min, to which hot complete medium was added using a pipette for scattering over the tissues. The remaining tissue was separated using a sterile stainless-steel mesh (100–200 mm). Mononuclear cell suspension was obtained by means of centrifugation.

Flow cytometry

Mononuclear cells (MSCs) were isolated from the bone marrow, induced membrane, and peripheral blood, cultured, and sorted by conducting FACS Vantage SE flow cytometry (Becton Dickinson and Company, NJ, USA). In details, the obtained cells were then re-suspended in PBS supplemented with 0.1% FBS and 0.5% NaN_3, centrifuged, and rinsed. After re-suspension, the cells were incubated with antibodies specific to CD29, CD34, CD44, and CD105 (AbD Serotec, Oxford, UK) at room temperature in conditions devoid of light for 30 min. The procedures were conducted as per the manufacturer's instructions. The supernatant was discarded and the precipitate was rinsed in PBS. After that, the precipitate was centrifuged at 1000 rpm for 5 min and the supernatant was removed after centrifugation. The centrifugation was repeated for three times. The harvested precipitate was re-suspended in 300 µl PBS. Flow cytometry was conducted after re-suspension. Before testing, the instrument was sterilized under 30 min ultraviolet irradiation, while the flow tubes were sterilized by hypochlorous acid. Sorting parameters were set based on the forward scatter (FSC), side scatter (SSC), and size of the cells. The separator was installed where the cells were sorted. Cells with the largest volume and quantity and most intra-cellular granules were selected as target cells for further experimentation.

Immunofluorescence

Bone marrow and induced membrane were fixed, decalcified, and prepared into frozen slices. Mononuclear cells from peripheral blood were cultured on the slide. Then, 0.5 Sudan black B diluted with 75% alcohol was dripped onto the slide, followed by water rinsing. Next, the slide was rinsed using Tween 20 (1000 ml PBS + 0.2 ml Tween 20) 3 times (5 min each time). After 5 PBS rinses, the slide was blocked using 1% BSA in the humidity chamber at 37 °C for 30 min. Then, the side was incubated with the SDF-1 monoclonal

primary antibody (1:10,000) at 4 °C overnight. After a rinse with PBS, the slide was incubated with the goat-anti-mouse fluorescent secondary antibody (1:1000) at 37 °C for 30 min–1 h, followed by three PBS rinses. Next, the slide was stained with 4′,6-diamidino-2-phenylindole (DAPI, 5 μg/ml) for 2 min. SDF-1 expression was observed immediately under a laser scanning confocal microscope (LSCM, Beijing Precise Instrument Co., Ltd., Beijing, China).

RNA extraction and reverse transcription quantitative polymerase chain reaction (RT-qPCR)

Total RNA was extracted from the bone marrow tissues and BMSCs of rats in the BG model using the TRIzol kit (15596-018, Invitrogen, Carlsbad, CA, USA) in strict accordance with the provided instructions. The purity and concentration of RNA were measured, respectively. Reverse transcription was performed using the PrimeScript TMRT reagent Kit (RRO37A, Takara Biotechnology Ltd., Kyoto, Japan) in strict accordance with the provided instructions. The reaction conditions were as follows: at 37 °C for 15 min (reverse transcription) and at 85 °C for 5 s (reverse transcriptase inactivation). Fluorescent quantitation PCR was conducted based on provided instructions of the SYBR® Premix Ex Taq™ II kit (Takara Biotechnology Ltd., Kyoto, Japan) using the ABI PRISM® 7300 system (ABI Company, Oyster Bay, NY, USA). The reaction conditions were as follows: predenaturation at 95 °C for 4 min followed by 40 cycles of denaturation at 94 °C for 30 s, annealing at 58 °C for 30 s, and extension at 72 °C for 1 min. Glyceraldehyde-3-phosphate dehydrogenase (GAPDH) was regarded as an internal control. Primer sequences are depicted in Table 1. The $2^{-\Delta C_t}$ method was adopted to calculate the target gene expression using a formula as $\Delta C_t = C_{\text{ttarget gene}} - C_{\text{tGAPDH}}$ [17]. The experiment was repeated three times independently.

Table 1 The primer sequences of SDF-1, CXCR4, BMP-2, Runx2, and GAPDH for RT-qPCR

Gene	Primer sequence (5′–3′)
SDF-1	F: TTGCCAGCACAAAGACACTCC
	R: CTCCAAAGCAAACCGAATACAG
CXCR4	F: TGACTCCAACAAGGAACCCTGC
	R: CGAAGATGATGTCAGGGATAGTC
BMP-2	F: AGCAGGTGGGAAAGTTTTGA
	R: CTCGTCAAGGTACAGCATCG
Runx2	F: GGACCGCCTCCTTCCAACT
	R: TCACTCGC CTCCGTCTACC
OPN	F: CATCAGAGCCACGAGTTTCA
	R: TCAGGGCCCAAAACACTATC
GAPDH	F: CCCCTGGCCAAGGTCATCCA
	R: CGGAAGCCATGCCAGTGAG

RT-qPCR reverse transcription quantitative polymerase chain reaction, *SDF-1* stromal cell-derived factor-1, *CXCR4* C-X-C motif chemokine receptor 4, BMP-2, bone morphogenetic protein-2, Runx2, runt-related transcription factor 2, GAPDH glyceraldehyde-3-phosphate dehydrogenase, *OPN* osteopontin, *F* forward, *R* reverse

Western blot analysis

Total protein was extracted from fresh bone marrow of rats in the BG model using the Radio-Immunoprecipitation Assay (RIPA) kit (R0010, Beijing Solarbio Life Sciences Co., Ltd., Beijing, China). The total protein concentrations were measured by bicinchoninic acid method. Next, 10% sodium dodecyl sulfate–polyacrylamide gel electrophoresis gel was conducted to separate proteins, and the proteins on the gel were transferred onto a nitrocellulose membrane. The nitrocellulose membrane was blocked in 5% skimmed milk (dissolved by tris-buffered saline) at room temperature for 1 h. Then, the membranes were incubated with the following diluted primary antibodies (diluted by 1 × TBST containing 5% skimmed milk) overnight at 4 °C: rabbit anti SDF-1 (1:10,000, ab9797), CXCR4 (1:100, ab124824), bone morphogenetic protein-2 (BMP-2, 1:500, ab14933) and runt-related transcription factor 2 (Runx2, 1:1000, ab23981), osteopontin (OPN, 1:1000, ab8448), and GAPDH (1:500, ab8245). The samples were rinsed with tris-buffered saline tween 20 (TBST) three times (10 min each time). The secondary goat-anti-rabbit IgG antibody (1:3000, ab6712) marked by horseradish peroxidase (HRP) was added to all samples and incubated. The aforementioned antibodies were purchased from Abcam (Cambridge, UK). The proteins were visualized using the enhanced chemiluminescence (ECL) reagent (WBKLS0500, Pierce, Rockford, IL, USA). GAPDH was regarded as an internal reference. The images of the gels were captured under a Bio-Rad Gel Doc EZ Imager (Bio-Rad, Hercules, CA, USA). The gray value of target band was quantified by ImageJ software.

Wound-healing assay

After infection of the BMSCs for 24 h, surface wounds of the cells were vertically scratched using a 200 μl pipette. Then, the cells were rinsed twice with serum-free medium, with removal of the cell debris. The cells were photographed under an inverted microscope, which was marked as 0 h. The cells were further incubated with serum-free medium at 37 °C with 5% CO_2 for 24 h. The scratch healing was observed at the same observation point and documented. The migration rate was calculated by measuring the scratch width of five points.

Statistical analysis

Data analysis was conducted using the SPSS 22.0 software (IBM Corp, Armonk, NY, USA). Measurement data were illustrated as mean ± standard deviation. The measurement data were tested for normality using the Kolmogorov–Smirnov test. If data conformed to normal distribution, statistical analysis among multiple groups was conducted using one-way analysis of variance, followed by Tukey's post hoc test. Comparison for different time points was conducted by repeated-measures analysis of variance, followed by Tukey's post hoc test. A value of $p < 0.05$ was indicative of significant results.

Results

Rat models of BD-IM and BG were successfully established

A total of 96 Wistar rats along with 60 SDF-1-knockout (SDF-$1^{-/-}$) rats were selected for establishment of BD model (Fig. 1b). Forty min post-operation, the modeled rats were awoken for observation of a limited range of left limb movement; however, no apparent inflammatory reactions were recorded. Approximately 1 week later, the rats moved freely in the cage with adequate healing of their respective wounds. X-ray examinations were conducted on the left femur before the rats were euthanized using carbon dioxide asphyxiation to observe the repair conditions of BD. The X-ray films (Fig. 1a) showed the formation of fibers in the central area and osteotylus in the peripheral region in BD rats, providing the verification for successful establishment of rat models.

The migration of MSCs in the induced membrane to damaged bone tissues

MSCs were isolated from the rats and the expression of MSCs surface markers (CD29, CD34, CD44, and CD105) was detected using flow cytometry. As shown in Fig. 2, MSCs exhibited high levels of CD29, CD44, and CD105 (96.4%, 96.1%, and 97.3%, resp.) along with a drastically low expression of CD34 (0.9%), thereby suggesting the successful isolation of MSCs.

The number of MSCs in peripheral blood, induced membrane, and bone marrow of rats from the BD-IM model is illustrated in Fig. 3. In comparison with the control group, the SDF-$1^{-/-}$ group had a lower number of MSCs, while the SDF-1 group had more MSCs (both $p < 0.05$). On days 1 and 3 after model establishment, the quantity of MSCs was the largest within the bone marrow, while the lowest quantity was observed in peripheral blood (all $p < 0.05$).

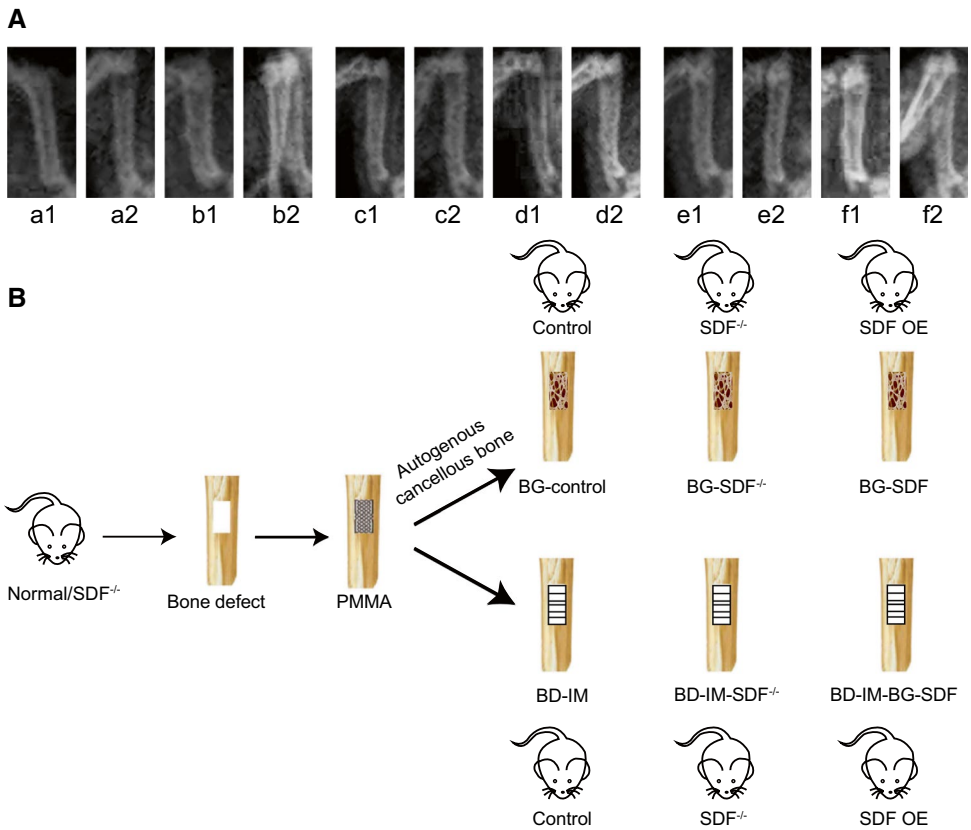

Fig. 1 X-ray scanning of the left femur provided confirmation of successful establishment of BD-IM and BG models. **a** a1, b1, c1, d1, e1, and f1 refer to the X-ray images of femur of rats in the BG control, BG SDF-$1^{-/-}$, BG SDF-1, BD-IM control, BD-IM SDF-$1^{-/-}$, and BD-IM SDF-1 groups, respectively, on day 14; a2, b2, c2, d2, e2, and f2 refer to the X-ray images of femur of rats in the BG control, BG SDF-$1^{-/-}$, BG SDF-1, BD-IM control, BD-IM SDF-$1^{-/-}$, and BD-IM SDF-1 groups on day 28. **b** Schematic map of BD-IM and BG modeling in SDF-$1^{-/-}$ and SDF-1 overexpressed rats. *BG* bone graft, *BD-IM* bone defect-induced membrane

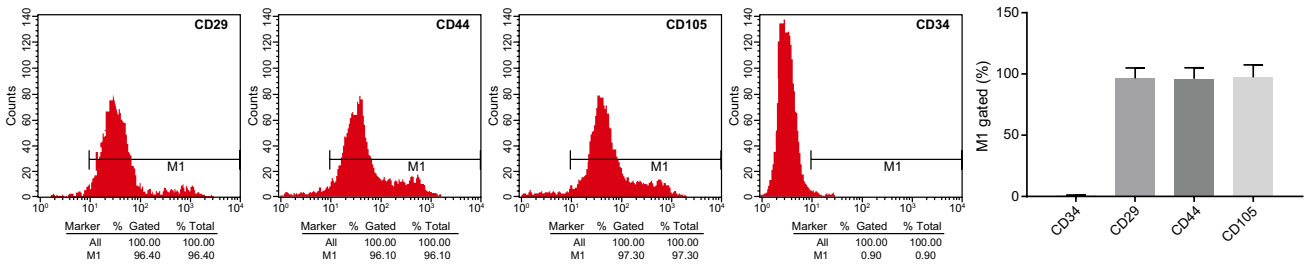

Fig. 2 Flow cytometric data show the expression of surface markers in the isolated MSCs and the positive rates of surface markers. CD29, CD44, and CD105 were highly-expressed, while that of CD34 was poorly expressed in MSCs at passage 3. *MSCs* mesenchymal stem cells

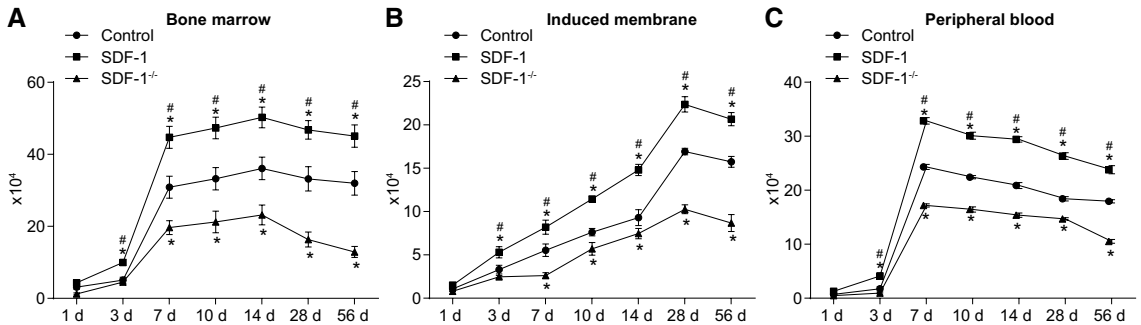

Fig. 3 The number of MSCs in BD-IM rats is increased by SDF-1 overexpression and MSCs are mainly recruited in the induced membrane. **a** The number of MSCs in the bone marrow on different days. **b** The number of MSCs in the induced membrane on different days. **c** the number of MSCs in the peripheral blood on different days. The data were regarded as measurement data. Comparison at different time points among groups was performed by repeated-measures analysis of variance, followed by Tukey's post hoc test. The experiment was conducted three times independently. $^{*}p<0.05$ compared with the control group. $^{\#}p<0.05$ compared with the SDF-$1^{-/-}$ group. *MSCs* mesenchymal stem cells, *SDF-1* stromal cell-derived factor 1, *BD-IM* bone defect-induced membrane

On days 7, 10, 14, 28, and 56, most MSCs in bone marrow, but least MSCs from the induced membrane were observed (all $p<0.05$). As time prolonged, the amount of MSCs in bone marrow was significantly increased, which peaked on the 14th day (Fig. 3a). However, the most MSCs from induced membrane were visualized on the 28th day, which was followed by a decreased amount (Fig. 3b). The number of MSCs from peripheral blood was conspicuously raised on days 1 and 3, which peaked on day 7, but gradually decreased thereafter (Fig. 3c). These findings highlighted the ability of the induced membrane to concentrate large quantities of MSCs.

The number of MSCs in the BG model is illustrated in Fig. 4. In contrast to the BG control group, the BG SDF-$1^{-/-}$ group illustrated a lower number of MSCs, while the BG SDF-1 group presented with an elevated number of MSCs (both $p<0.05$). On day 1 and 3 post-modeling, the quantity of MSCs was higher in the induced membrane than that observed in the bone marrow and peripheral blood; however, most MSCs were found in the bone marrow among the three groups (all $p<0.05$). On days 7, 10, 14, 28, and 56, more MSCs were observed in bone marrow but less in the induced membrane than those in peripheral blood in all the three groups (all $p<0.05$). The number of MSCs in bone marrow gradually increased over time, which peaked on day 14 (Fig. 4a). The number of MSCs from the induced membrane peaked on day 1 and slowly decreased in the following days (Fig. 4b). The number of MSCs peaked on day 7 in the peripheral blood, and reduced thereafter (Fig. 4c). These findings demonstrated that MSCs in the induced membrane could migrate to the damaged bone tissue gradually over time. Figures 3b and 4b clearly exhibit that MSCs could be concentrated in the induced membrane to a certain extent and then be transferred to the damaged bone marrow.

SDF-1 up-regulated osteogenesis-related genes by activating the SDF-1/CXCR4 signal pathway

For the purposes of analyzing the mechanisms and functions of SDF-1 in osteogenesis, mRNA expression of osteogenesis-related genes (BMP-2, Runx2, and OPN) was measured in the provided bone marrow tissues of rats in the BG model. The RT-qPCR results (Fig. 5) revealed that SDF-1 was knocked out, and the mRNA expression of CXCR4, BMP-2,

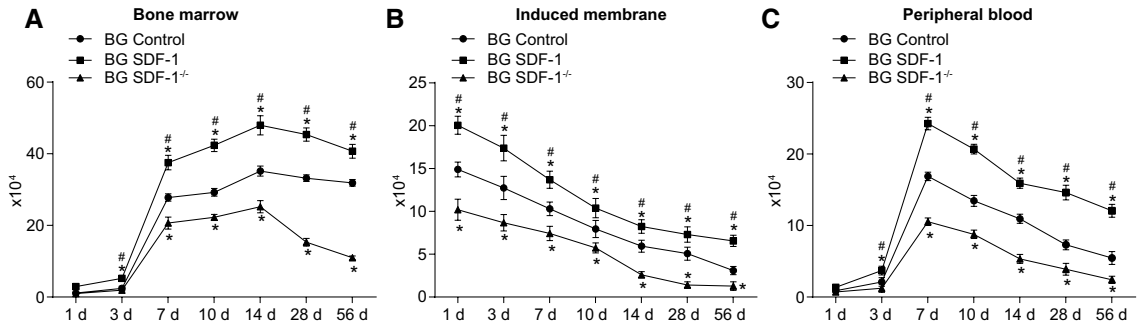

Fig. 4 The number of MSCs in BG rats is increased by SDF-1 overexpression. **a** The number of MSCs in bone marrow on different days. **b** The number of MSCs in induced membrane on different days. **c** The number of MSCs in peripheral blood on different days. The data were regarded as measurement data. Comparison at different time points among groups was performed by repeated-measures analysis of variance, followed by Tukey's post hoc test. The experiment was conducted three times independently. $^{*}p<0.05$ compared with the BG control group. $^{\#}p<0.05$ compared with the BG SDF-$1^{-/-}$ group. *MSCs* mesenchymal stem cells, *SDF-1* stromal cell-derived factor 1, *BG* bone graft

Runx2, and OPN was inhibited in the SDF-$1^{-/-}$ group, but elevated in the SDF-1 group in comparison to the control group (all $p<0.05$), with the highest SDF-1 and CXCR4 mRNA expression evident on day 7 and highest BMP-2, Runx2, and OPN mRNA expression on day 14.

The functional mechanism for the induced membrane on those osteogenic proteins during the repair process of BD was subsequently analyzed using Western blots and manifested by its regulatory roles in the expression of SDF-1/CXCR4 axis-related proteins (Fig. 6). In comparison with the control group, the SDF-$1^{-/-}$ group exhibited no SDF-1 protein expression and notably lower protein expression of CXCR4, BMP-2, Runx2, and OPN in the bone marrow tissues; however, the SDF-1 group had elevated protein expression of SDF-1, CXCR4, BMP-2, Runx2, and OPN in the bone marrow tissues (all $p<0.05$). SDF-1 and CXCR4 protein reached their highest levels on day 7. Seven days later, the highest BMP-2, Runx2, and OPN protein expression was documented in the bone marrow tissues. The results demonstrated that up-regulated SDF-1 could facilitate the activation of the SDF-1/CXCR4 axis to elevate the levels of osteogenic proteins in the bone marrow tissues.

These findings provided ascertained that SDF-1 up-regulation could mobilize the host cells to migrate to the BD area thus participating in osteogenesis through its compelling role in the activation of the SDF-1/CXCR4 axis upon employing the induced membrane technique to repair BD.

Up-regulated SDF-1 promoted the transfer of MSCs to the damaged bone marrow tissues

To determine the SDF-1 expression in the bone marrow tissues of the BD-IM and BG models, LSCM was conducted and results are exhibited in Fig. 7. In relation to the BD-IM model (Fig. 7a, c), no expression of SDF-1 was observed in the SDF-$1^{-/-}$ group and higher SDF-1 expression was detected in the SDF-1 group than that observed in the control group (both $p<0.05$). SDF-1 level in the bone marrow tissue and peripheral blood reached its zenith on day 7, while the level in the induced membrane tissue peaked on day 28.

As shown in Fig. 7b, d, compared with the BG control group, no expression of SDF-1 was detected in the BG SDF-$1^{-/-}$ group, but up-regulated SDF-1 expression was observed in the BG SDF-1 group (both $p<0.05$). SDF-1 level in the bone marrow tissue as well as the peripheral blood peaked on day 7, while the peak was observed on day 1 in the induced membrane tissue. Considering the number of MSCs at different time points, up-regulated SDF-1 could potentially stimulate the mobilization and migration of MSCs.

SDF-1 promoted MSC migration with the application of induced membrane

Finally, the effect of the induced membrane on migration of MSCs was detected by Transwell assay and the results are presented in Fig. 8. In comparison with the control group, the SDF-$1^{-/-}$ group exhibited a decreased migration rate of MSCs, yet the SDF-1 group presented with an elevated migration rate (both $p<0.05$). The migration rate of MSCs was lower in the BG SDF-$1^{-/-}$ group but higher in the BG SDF-1 group than that observed in the BG control group (both $p<0.05$). Hence, SDF-1 overexpression could promote the migration of MSCs in BD repair. In comparison to the control group, the BG control group enhanced the migration potential ($p<0.05$), suggesting that the induced membrane could extensively enhance the migration ability of MSCs.

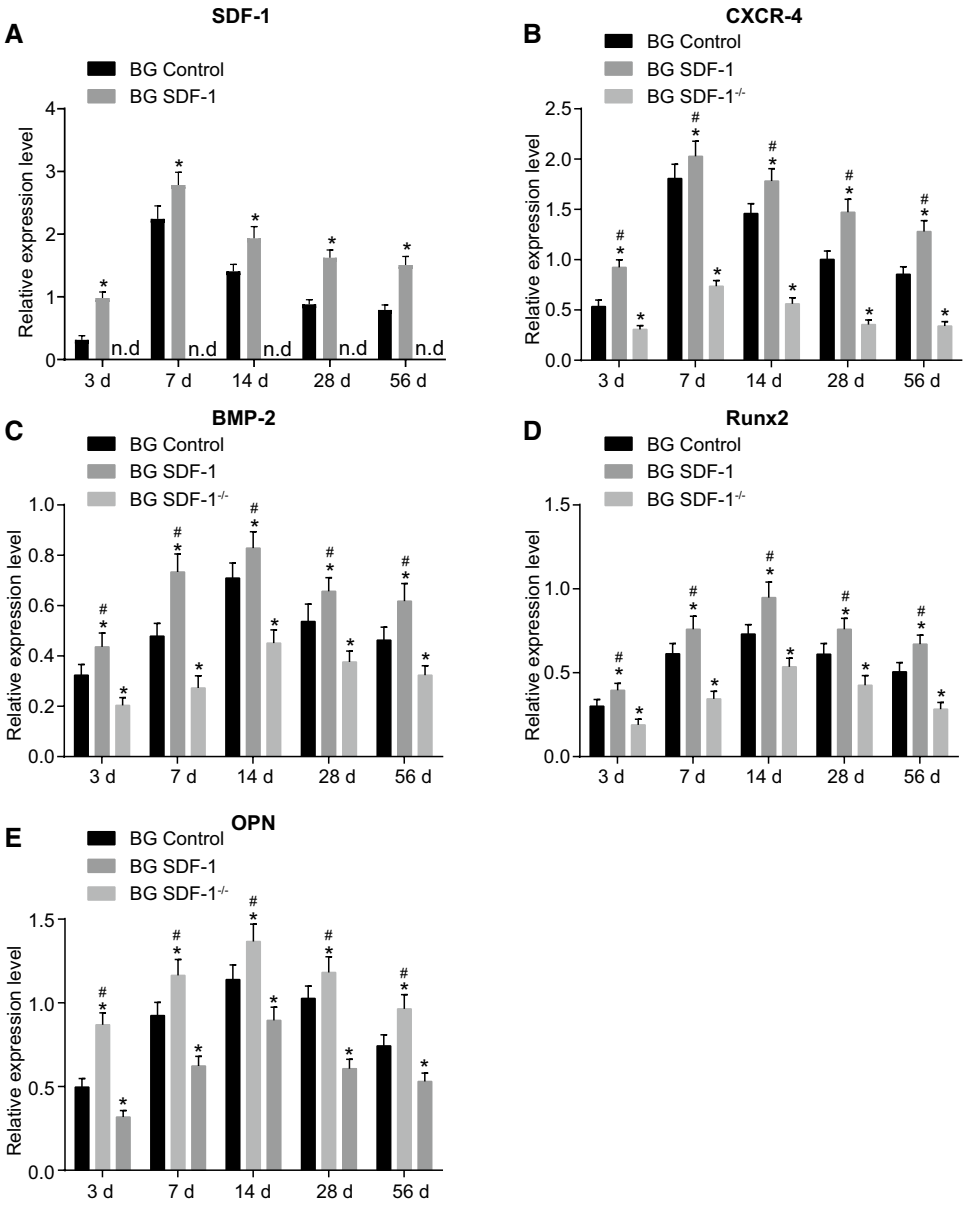

Fig. 5 SDF-1 increased the relative mRNA levels of CXCR4, BMP-2, Runx2, and OPN in the bone marrow tissues of BG rats. **a** SDF-1 mRNA level in the bone marrow tissues determined by RT-qPCR (no SDF-1 was detected in the SDF-1$^{-/-}$ group at different time points). **b** CXCR4 mRNA level in the bone marrow determined by RT-qPCR. **c** BMP-2 mRNA level in the bone marrow tissues determined by RT-qPCR. **d** Runx2 mRNA level in the bone marrow tissues determined by RT-qPCR. **e** OPN mRNA level in the bone marrow tissues determined by RT-qPCR. The data were regarded as measurement data. Comparison at different time points was performed by repeated-measures analysis of variance, followed by Tukey's post hoc test. The experiment was conducted three times independently. $^{*}p < 0.05$ compared with the BG control group. $^{\#}p < 0.05$ compared with the BG SDF-1$^{-/-}$ group. *SDF-1* stromal cell-derived factor 1, *CXCR4* C-X-C motif chemokine receptor 4, *BMP-2* bone morphogenetic protein-2, *Runx2* runt-related transcription factor 2, *OPN* secreted phosphoprotein 1, *BG* bone graft, *RT-qPCR* reverse transcription quantitative polymerase chain reaction

Discussion

The concept of induced membrane, serving as a biological chamber, has provided a new insight for the clinical management of BDs by preventing bone-graft resorption in addition to promoting revascularization and consolidation [15]. Additionally, SDF-1, a ligand for CXCR4, which is released from various cell types in bone marrow, has been reported to expedite the progression of BD healing [18, 19]. Hence, we extensively investigated the potential role of SDF-1 in the induced membrane treatment for BD repair through involvement of its effects on BMSCs via the SDF-1/CXCR4 axis.

A significant finding of the present study highlighted that BMSCs concentrated in the induced membrane could successfully migrate to the injured part of the bone marrow as a modality followed by stimulated facilitation of the healing process of BD. A group of Chinese researchers have asserted that any changes in the quantity of BMSCs could ultimately have a negative impact on fractural healing, which may cause the occurrence of pathological changes [20]. Masquelet and Begue have flagged the potential association of the migration potential of osteoblasts with osteogenesis in BD [15]. Importantly, an injury could stimulate BMSCs to transfer to the affected area [21]. As previously highlighted, the migration ability of MSCs can be enhanced by SDF-1 especially

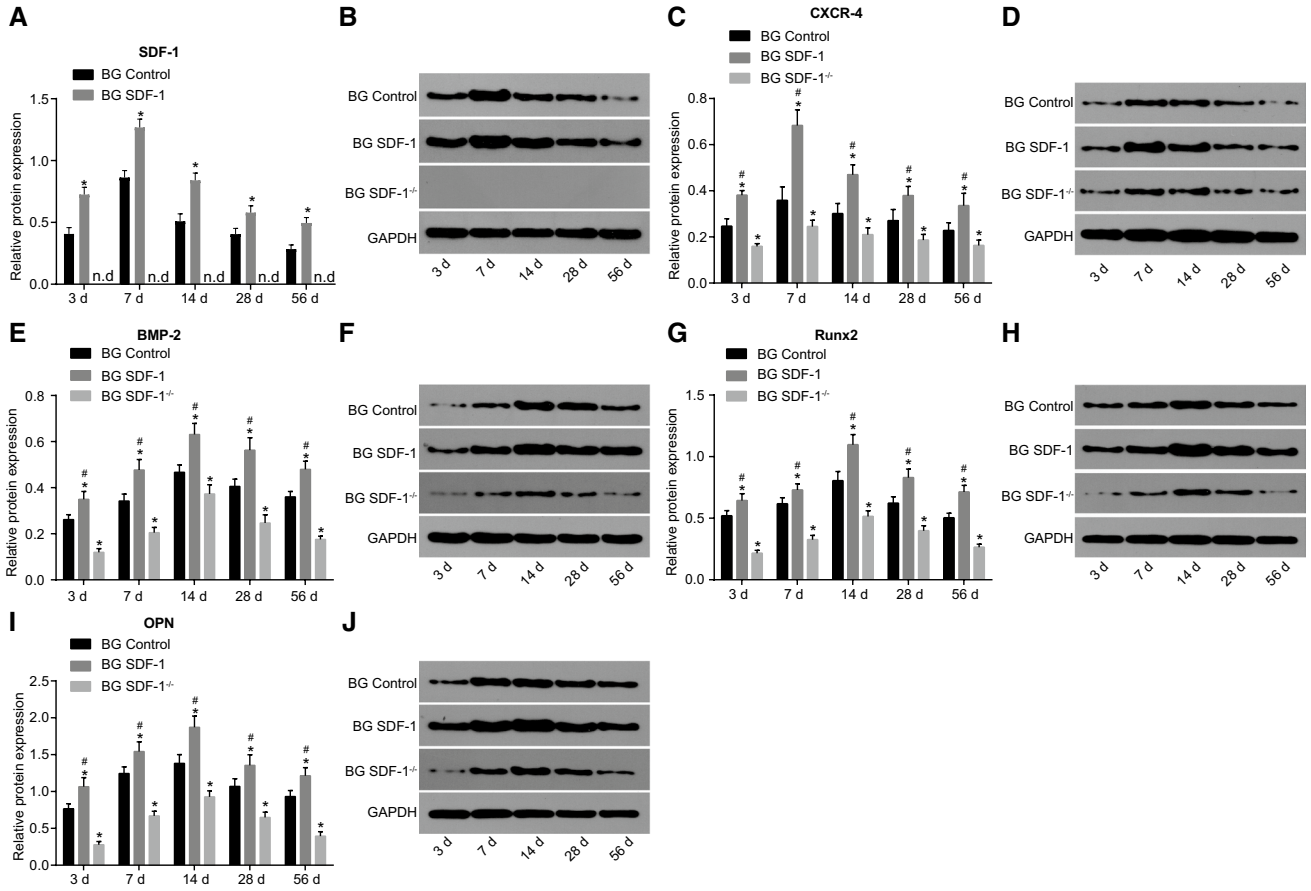

Fig. 6 SDF-1 elevated the protein levels of CXCR4, BMP-2, Runx2, and OPN in the bone marrow tissues of BG rats. **a** The protein level of SDF-1 in the bone marrow tissues (no SDF-1 was detected in the SDF-$1^{-/-}$ group at different time points); **b** representative Western blot bands of SDF-1 protein in the bone marrow tissues (no SDF-1 was detected in the SDF-$1^{-/-}$ group at different time points); **c** CXCR-4 protein level in the bone marrow tissues; **d** representative Western blot bands of CXCR-4 protein in the bone marrow tissues; **e** BMP2 protein level in the bone marrow tissues; **f** representative Western blot bands of BMP2 protein in the bone marrow tissues; **g** RUNX2 protein level in the bone marrow tissues; **h** representative Western blot bands of RUNX2 protein in the bone marrow tissues; **i** the protein level of OPN in the bone marrow tissues; **j** representative Western blot bands of OPN protein in the bone marrow tissues. The data were regarded as measurement data. Comparison at different time points was performed by repeated-measures analysis of variance, followed by Tukey's post hoc test. The experiment was conducted three times independently. $^{*}p < 0.05$ compared with the BG control group. $^{\#}p < 0.05$ compared with the BG SDF-$1^{-/-}$ group. *SDF-1* stromal cell-derived factor 1, *CXCR4* C-X-C motif chemokine receptor 4, *BMP-2* bone morphogenetic protein-2, *Runx2* runt-related transcription factor 2, *OPN* secreted phosphoprotein 1, *GAPDH* glyceraldehyde-3-phosphate dehydrogenase, *BG* bone graft

[22]. Furthermore, an elevated expression of SDF-1 has been documented to positively impact the injury repair [23]. An experiment conducted on rats has reported that BMSCs overexpressing SDF-1 exhibit far greater extent of bone formation during the early healing stage of BD [24], which was in consistency with the findings of the current study, supporting that the up-regulation of SDF-1 may serve as an initiating factor for BMSCs mobilization and migration.

From the perspective of the SDF-1/CXCR4 axis, we determined the mRNA and protein expression of CXCR4, and osteogenesis-related factors (BMP-2, Runx2, OPN) and the observations substantiated that up-regulated SDF-1 mobilized the participation of various factors in osteogenesis at the lesion by facilitating the activation of the SDF-1/CXCR4 pathway. Marquez-Curtis and Janowska-Wieczorek have highlighted the potential of the SDF-1/CXCR4 axis as a pivotal pathway for MSCs to migrate especially to the injured area where abundant SDF-1 would amplify the involvement of CXCR4-positive cells [25]. Meanwhile, the SDF-1/CXCR4 axis is considered to function as a vital system whereby circulating stem cells are guided to the injury site [26]. CXCR4 has been delineated as a key regulator for the mobilization of stem cells [27]. Evidence elucidating the role of BMP-2 was flagged by Dumic-Cule et al., stating that the involvement of BMP-2 may lead

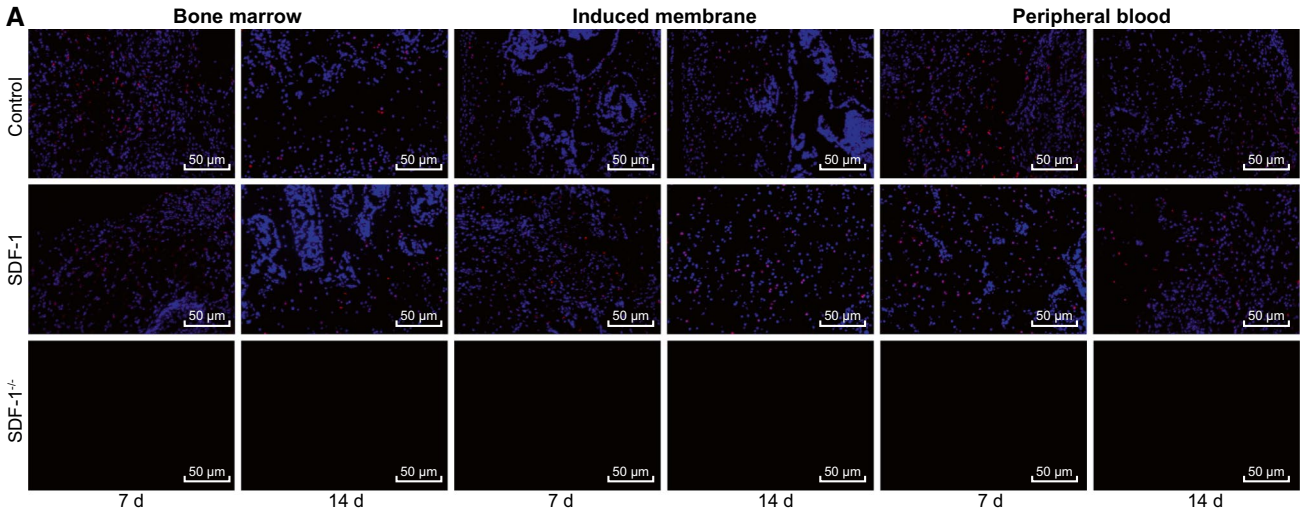
A
Bone marrow
Induced membrane
Peripheral blood
Control
SDF-1
SDF-1-/-
50 μm
7 d
14 d

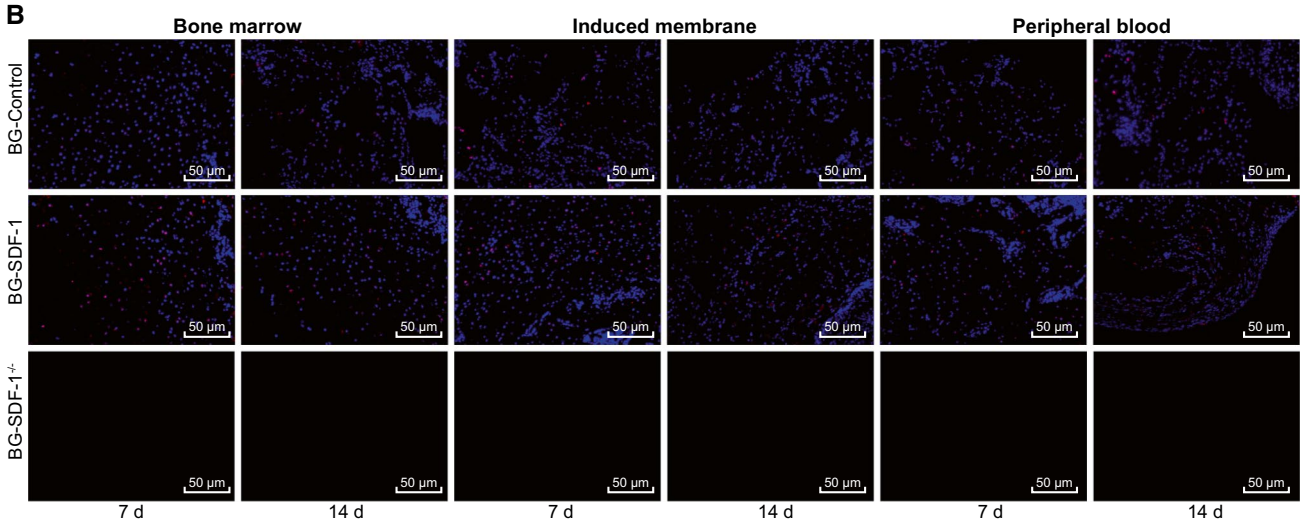
B
Bone marrow
Induced membrane
Peripheral blood
BG-Control
BG-SDF-1
BG-SDF-1-/-
50 μm
7 d
14 d

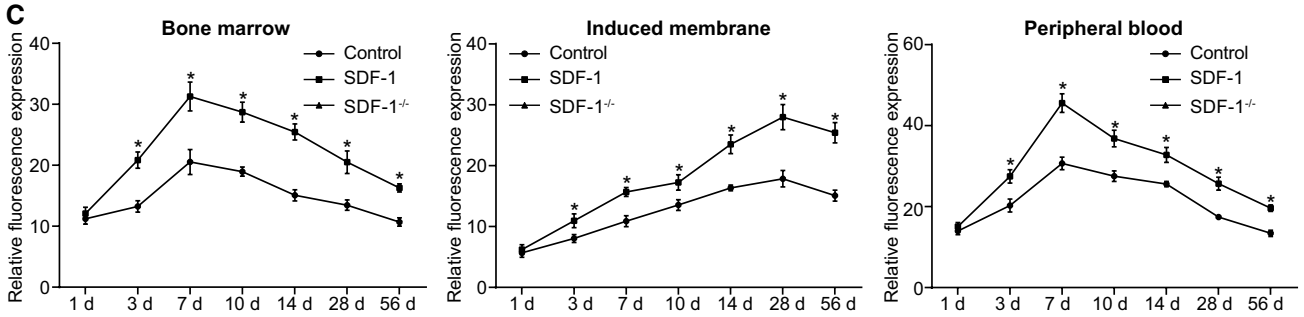
C
Bone marrow
Induced membrane
Peripheral blood
Control
SDF-1
SDF-1-/-
Relative fluorescence expression
1 d
3 d
7 d
10 d
14 d
28 d
56 d

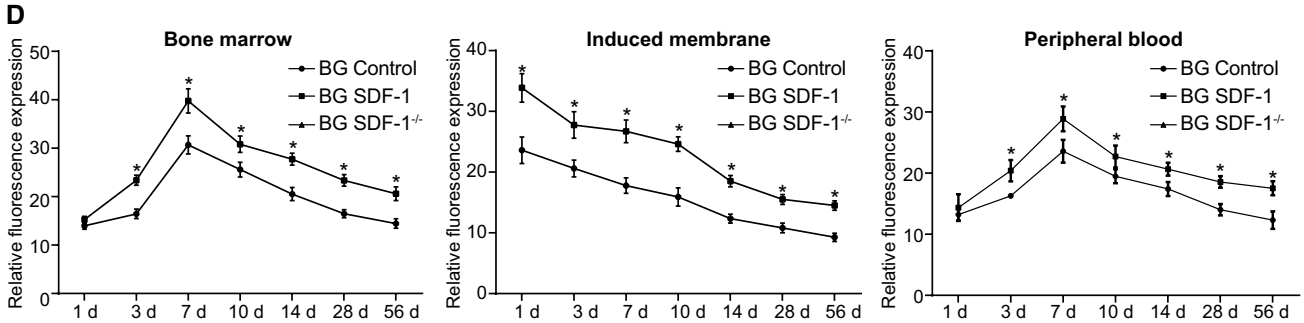
D
Bone marrow
Induced membrane
Peripheral blood
BG Control
BG SDF-1
BG SDF-1-/-
Relative fluorescence expression
1 d
3 d
7 d
10 d
14 d
28 d
56 d

◂**Fig. 7** Increased SDF-1 expression promotes the transfer of BMSCs to damaged bone marrow tissues. **a** Laser scanning confocal microscopic observation of SDF-1 expression in the bone marrow, induced membrane, and peripheral blood of the control, SDF-$1^{-/-}$ and SDF-1-overexpressed BD-IM rats on day 7 and 14. **b** Laser scanning confocal microscopic observation of SDF-1 expression in the bone marrow, induced membrane, and peripheral blood of the control, SDF-$1^{-/-}$ and SDF-1-overexpressed BG rats on day 7 and 14. **c** expression of SDF-1 in the bone marrow, induced membrane, and peripheral blood of the control and SDF-1-overexpressed BD-IM rats on different days (no SDF-1 was detected in the SDF-$1^{-/-}$ group at different time points). **d** expression of SDF-1 in the bone marrow, induced membrane, and peripheral blood of the control and SDF-1-overexpressed BG rats on different days. The data were regarded as measurement data, expressed by mean ± standard deviation. Comparison at different time points was performed by repeated-measures analysis of variance, followed by Tukey's post hoc test. The experiment was conducted three times independently. *$p < 0.05$ compared with the control or BG control group. *BD-IM* bone defect-induced membrane, *BG* bone graft, *SDF-1* stromal cell-derived factor 1

to a series of reactions related to cells and further contribute to the repair of BD [28]. Runx2, belonging to the family of runt transcription factors, is a crucial gene for the differentiation of the osteoblast lineage [29]. OPN, also known as sialoprotein-1, is a member of the small integrin-binding ligand N-linked glycoprotein (SIBLING) family and is regarded to affect bone morphogenesis as well as bone remodeling [30]. Factors SDF-1 and OPN were both observed to be up-regulated before any evident accumulation of monocytes in the adventitia pulmonary arteries [31]. In a study conducted by Chen et al., if Runx2 is found to be absent in mice, bone formation and osteoblast maturation would fail as a consequence [32]. Similarly, Qin et al., have conducted an experiment on human BMSCs and found that medium supplemented with BMSCs would promote osteoblastic differentiation by higher expression levels of related genes, including OPN and Runx2, which may serve as a valuable tool for bone regeneration [33]. The aforementioned findings indicated the notion that up-regulated SDF-1 promoted the migration of MSCs to damaged areas in bone marrow and probably enhanced osteoblastic differentiation potentials of MSCs which may facilitate bone regeneration.

Collectively, our key findings suggested that SDF-1 mediated BMSC mobilization and migration in rat model of BD treated with the induced membrane technique by activating the SDF-1/CXCR4 axis, More importantly, although our provisional results display the positive influence of SDF-1 on BMSCs, thorough investigations in the future are still required to reveal the potential implications of these findings in a clinical setting.

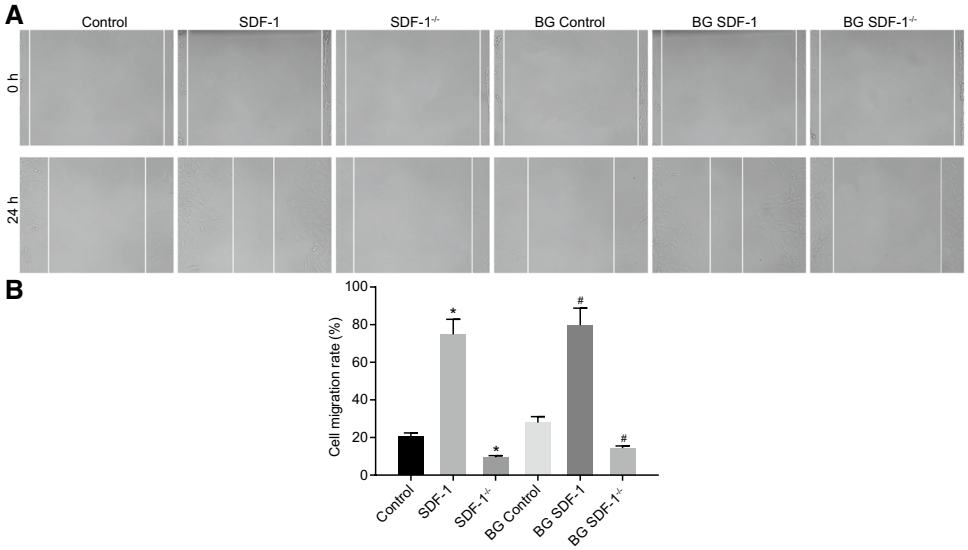

Fig. 8 Induced membrane technique or SDF-1 promotes the migration of BMSCs. **a** Representative scratch images at 0 h and 14 h. **b** Migration rates of BMSCs from control, SDF-1-overexpressed and SDF-$1^{-/-}$ BD-IM or BG rats. The data were regarded as measurement data and expressed by mean ± standard deviation. Comparison between multiple groups was performed by one-way analysis of variance, followed by Tukey's post hoc test. The experiment was conducted three times independently. *$p < 0.05$ compared with the control group. #$p < 0.05$ compared with the BG control group. *SDF-1* stromal cell-derived factor 1, *BG* bone graft, *BMSCs* bone marrow-derived mesenchymal stem cells, *BD* bone defect

Acknowledgements We acknowledge and appreciate our colleagues for their valuable efforts and comments on this paper.

Funding None.

Compliance with ethical standards

Conflict of interest All authors have no conflicts of interest.

References

1. Zhu W, Wang D, Xiong J, Liu J, You W, Huang J, Duan L, Chen J, Zeng Y (2015) Study on clinical application of nano-hydroxyapatite bone in bone defect repair. Artif Cells Nanomed Biotechnol 43:361–365
2. Wiese A, Pape HC (2010) Bone defects caused by high-energy injuries, bone loss, infected nonunions, and nonunions. Orthop Clin N Am 41:1–4 **(table of contents)**
3. Eskander R, Ji T, Wang Y, Sun K, Hoang BH, Guo W (2014) Can surgical management of bone metastases improve quality of life among women with gynecologic cancer? World J Surg Oncol 12:250
4. Xu N, Ye X, Wei D, Zhong J, Chen Y, Xu G, He D (2014) 3D artificial bones for bone repair prepared by computed tomography-guided fused deposition modeling for bone repair. ACS Appl Mater Interfaces 6:14952–14963
5. Auregan JC, Begue T (2014) Induced membrane for treatment of critical sized bone defect: a review of experimental and clinical experiences. Int Orthop 38:1971–1978
6. Kishi T, Karger C, Schneider L, Fitoussi F, Masquelet AC (2012) French Society of Orthopaedic S Traumatology. Treatment of posttraumatic bone defects by the induced membrane technique. Orthop Traumatol Surg Res 98:97–102
7. Marquez-Curtis LA, Janowska-Wieczorek A (2013) Enhancing the migration ability of mesenchymal stromal cells by targeting the SDF-1/CXCR4 axis. Biomed Res Int 2013:561098
8. Masyuk M, Brand-Saberi B (2015) Recruitment of skeletal muscle progenitors to secondary sites: a role for CXCR4/SDF-1 signalling in skeletal muscle development. Results Probl Cell Differ 56:1–23
9. Nagasawa T (2014) CXC chemokine ligand 12 (CXCL12) and its receptor CXCR4. J Mol Med (Berl) 92:433–439
10. Song F, Sun H, Huang L, Fu D, Huang C (2017) The role of Pannexin3-modified human dental pulp-derived mesenchymal stromal cells in repairing rat cranial critical-sized bone defects. Cell Physiol Biochem 44:2174–2188
11. Sensebe L, Krampera M, Schrezenmeier H, Bourin P, Giordano R (2010) Mesenchymal stem cells for clinical application. Vox Sang 98:93–107
12. Fakhari S, Kalantar E, Nikzaban M, Hakhamneshi MS, Fathi F, Nikkhoo B, Rahmani MR, Beiraghdar M, Jalili A (2014) Effect of Helicobacter pylori infection on stromal-derived factor-1/CXCR4 axis in bone marrow-derived mesenchymal stem cells. Adv Biomed Res 3:19
13. Wang Y, Sun X, Lv J, Zeng L, Wei X, Wei L (2017) Stromal cell-derived factor-1 accelerates cartilage defect repairing by recruiting bone marrow mesenchymal stem cells and promoting chondrogenic differentiation. Tissue Eng Part A 23:1160–1168
14. Okada K, Kawao N, Yano M, Tamura Y, Kurashimo S, Okumoto K, Kojima K, Kaji H (2016) Stromal cell-derived factor-1 mediates changes of bone marrow stem cells during the bone repair process. Am J Physiol Endocrinol Metab 310:E15–E23
15. Masquelet AC, Begue T (2010) The concept of induced membrane for reconstruction of long bone defects. Orthop Clin N Am 41:27–37 **(table of contents)**
16. Peng WX, Wang L (2017) Adenovirus-mediated expression of BMP-2 and BFGF in bone marrow mesenchymal stem cells combined with demineralized bone matrix for repair of femoral head osteonecrosis in beagle dogs. Cell Physiol Biochem 43:1648–1662
17. Spinelli O, Pagani IS, Mattarucchi E, Pirrone C, Pigni D et al (2014) Genomic quantitative real-time PCR proves residual disease positivity in more than 30% samples with negative mRNA-based qRT-PCR in chronic myeloid leukemia. Oncoscience 1:510–521
18. Hirbe AC, Morgan EA, Weilbaecher KN (2010) The CXCR4/SDF-1 chemokine axis: a potential therapeutic target for bone metastases? Curr Pharm Des 16:1284–1290
19. Ho CY, Sanghani A, Hua J, Coathup M, Kalia P, Blunn G (2015) Mesenchymal stem cells with increased stromal cell-derived factor 1 expression enhanced fracture healing. Tissue Eng Part A 21:594–602
20. Li C, Ding J, Jiang L, Shi C, Ni S, Jin H, Li D, Sun H (2014) Potential of mesenchymal stem cells by adenovirus-mediated erythropoietin gene therapy approaches for bone defect. Cell Biochem Biophys 70:1199–1204
21. Nabil I, Mehanna RA, Attia N, Bary AA, Razek KA, Ahmed TA, Elsayed F (2015) The effect of bone marrow-derived mesenchymal stem cells and their conditioned media topically delivered in fibrin glue on chronic wound healing in rats. Biomed Res Int 2015:846062
22. Osugi M, Katagiri W, Yoshimi R, Inukai T, Hibi H, Ueda M (2012) Conditioned media from mesenchymal stem cells enhanced bone regeneration in rat calvarial bone defects. Tissue Eng Part A 18:1479–1489
23. Mamillapalli R, Wang X, Mutlu L, Du H, Taylor HS (2015) Chemoattraction of bone marrow-derived stem cells towards human endometrial stromal cells is mediated by estradiol regulated CXCL12 and CXCR4 expression. Stem Cell Res 15:14–22
24. Sanghani A, Ho CY, Hua J, Coathup M, Kalia P, Blunn G (2015) Mesenchymal stem cells with increased stromal cell-derived factor 1 expression enhanced fracture healing. Tissue Eng Part A 21:594–602
25. Janowska-Wieczorek A, Marquez-Curtis LA (2013) Enhancing the migration ability of mesenchymal stromal cells by targeting the SDF-1/CXCR4 axis. Biomed Res Int 2013:561098
26. Giannobile W, Jin Q (2014) SDF-1 enhances wound healing of critical-sized calvarial defects beyond self-repair capacity. PLoS ONE 9:e97035
27. Wei Y, Shi J, Xia J, Wang S, Wu J et al (2014) CXCL12-CXCR4 contributes to the implication of bone marrow in cancer metastasis. Future Oncol 10:749–759
28. Pecina M, Dumic-Cule I, Jelic M, Jankolija M, Popek I, Grgurevic L, Vukicevic S (2015) Biological aspects of segmental bone defects management. Int Orthop 39:1005–1011
29. Nakazato R, Takarada T, Tsuchikane A, Fujikawa K, Iezaki T, Yoneda Y, Hinoi E (2016) Genetic analysis of Runx2 function during intramembranous ossification. Development 143:211–218
30. Messina A, De Fusco C, Monda V, Viggiano E, Moscatelli F et al (2017) Osteopontin: relation between adipose tissue and bone homeostasis. Stem Cells Int 2017:4045238
31. Frid M, Burke DL, Kunrath CL, Karoor V, Anwar A et al (2009) Sustained hypoxia promotes the development of a pulmonary artery-specific chronic inflammatory microenvironment. Am J Physiol Lung Cell Mol Physiol 297:L238–L250
32. Yuan K, Chen J, Mao X, Miano JM, Wu H, Chen Y (2012) Serum response factor regulates bone formation via IGF-1 and Runx2 signals. J Bone Miner Res 27:1659–1668

33. Wang L, Qin Y, Gao Z, Chen G, Zhang C (2016) Bone marrow stromal/stem cell-derived extracellular vesicles regulate osteoblast activity and differentiation in vitro and promote bone regeneration in vivo. Sci Rep 6:21961